Research Reports

Research Reports

Numerical modelling techniques

The Numerical Modelling Techniques research stream develops innovative computational techniques and tools necessary to model offshore infrastructure, with a focus on developing computational algorithms capturing multi-phase sediment response, consolidation and strain rate effects in large deformation problems. In 2012, numerical modelling technology continued to build on developments in the mesh-free material point method (MPM) and large deformation finite element analysis (LDFEA) through the remeshing and interpolation technique with small strain method (RITSS). Researchers have also been investigating the potential of the LDFEA coupled Eulerian-Lagrangian method (CEL) available in the commercial version of Abaqus.

Breakthroughs in 2012 include new algorithms for soil-structure contact and strain rate dependency for the MPM, implantation of a coupled consolidation model in a LDFE framework implemented into Abaqus, programming refinements of the RITSS method in Abaqus to make LDFE accessible to non-programrs and a rate dependent model implemented into Abaqus CEL.

Numerical modelling of submarine landslides using the material point method (MPM)

PhD student Jiajie Ma has developed a new algorithm for the material point method (MPM), a finite element method based mesh-free method, to study submarine landslides. Submarine landslides pose considerable risk to pipelines and other offshore infrastructures in deep water, but sophisticated numerical modelling of these events is challenging as slides involve large deformation, multi-phase flow and soil-structure interaction. The material point method is potentially a valuable tool to overcome these issues and accurately model submarine slide kinematics and the effect on the seabed materials. Jiajie's main achievement in 2012 is developing a new contact algorithm for geotechnical applications that incorporates a penalty function and limiting shear stress for modelling frictional structure-soil contact. The algorithm has been validated by comparing results of flow around a T-bar with conventional LDFE results and limit analysis solutions in benchmark cases (Figure 37).

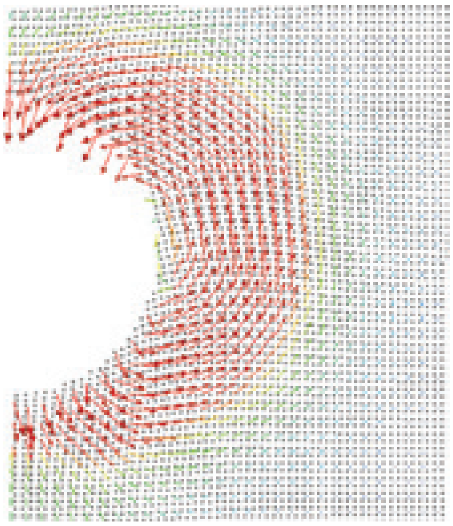

Figure 37: Soil velocity vectors around a smooth T-bar with new contact algorithm with new contact algorithm

Incorporation of a rate-dependent soil model for the material point method (MPM)

A softening and rate-dependent soil model was incorporated into open source MPM package Unitah by PhD student Youkou Dong. The model was verified in terms of pipe penetration in soft clay (Figure 38). A disadvantage of MPM is that its computational efficiency is much lower than conventional finite element methods. Youkou developed a simple technique in the Unitah package to save up to 50% effort for plane strain problems. The GPU programming is in progress for large-scale large deformation analysis, which can be applied to a range of large deformation problems.

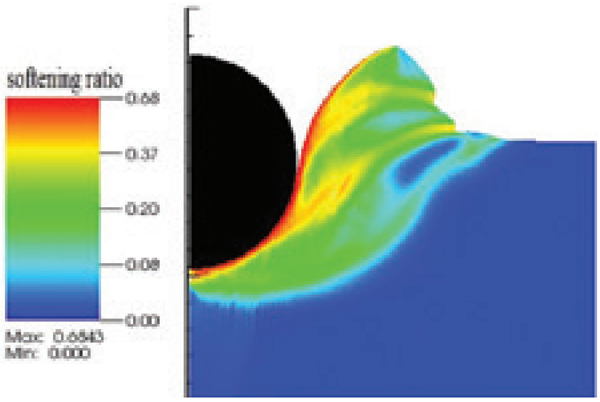

Figure 38: Softening ratio at pipe penetration depth of half diameter

Coupled large deformation finite element analysis (LDFEA) of partially embedded submarine pipelines

PhD student Santiram Chatterjee performed coupled pore-fluid large deformation finite element analyses to study the effects of consolidation beneath the partially embedded offshore pipelines. The large deformation formulation used for the analyses was developed in-house as part of his PhD studies. The results show the distribution of shear strength increase of the soil due to consolidation beneath a loaded pipe and that the lateral breakout resistance and the direction of pipe movement depend on the strength distribution of the soil around the pipe. It is shown that the pipe-soil interaction forces in the vertical and lateral direction can differ markedly from those predicted assuming undrained behaviour. Figure 39 shows contours of shear strength compared to the original undrained shear strength at an embedment level of w/D = 0.5 resulting from consolidation.

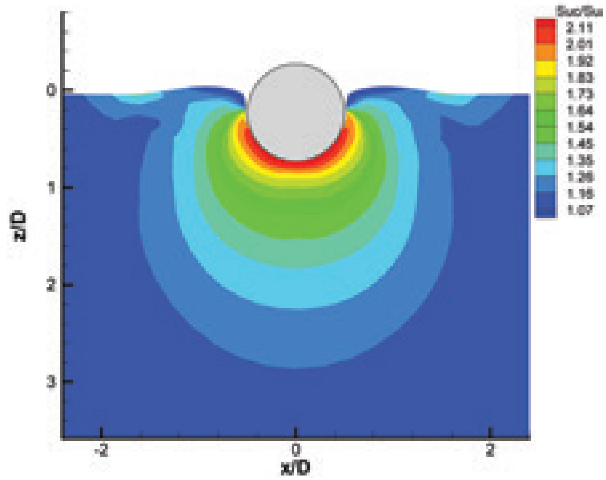

Figure 39: Increase in shear strength due to consolidation beneath partially embedded pipe

Implementation of an automated LDFE RITSS method into ABAQUS

Yinghui Tian implemented a large deformation finite element (LDFE) approach into the commercial package ABAQUS within the 'Remeshing and Interpolation Technique with Small Strain' (RITSS) framework. The prominent feature of this implementation is different from available methods in that no user coding is required to interpolate the results from old mesh to new mesh. In the new implementation, these processes are conducted within ABAQUS built-in functionality. This will significantly reduce the coding work and make the RITSS framework accessible for non-programrs. This simple approach has been validated against available publications, including the applications for T-bar, pipeline, shallow footing and plate anchor. Figure 40 shows the flow mechanism for deep penetration of T-bar (for smooth and rough contact, respectively).

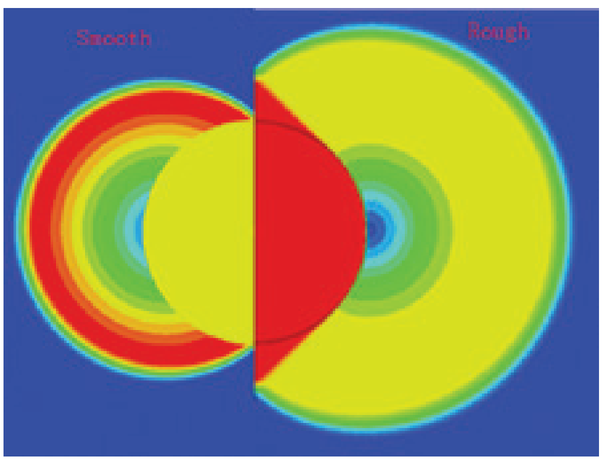

Figure 40: Flow mechanism around a T-bar from new LDFE implementation

Implementation of a strain dependent model into a Coupled Eulerian-Lagrangian (CEL) software

PhD student Jingbin Zheng, has incorporated the effect of strain softening and strain rate dependency of the undrained shear strength of clay into the Coupled Eulerian-Lagrangian (CEL) approach in ABAQUS/Explicit. In 2012, 3D large deformation finite element (LDFE) parametric analyses have been carried out to investigate the effects of seabed layer geometry and soil properties on the penetration resistance of a spudcan. Figure 41 shows the contour of undrained shear strength before and after the incorporation of strain softening and strain rate during spudcan penetration. The CEL results have been validated against centrifuge test data with excellent agreement obtained. The effect of strain softening and strain rate dependency has been shown to have significant influence not only on the magnitude of resistance mobilised but also on the form of load-displacement profile.

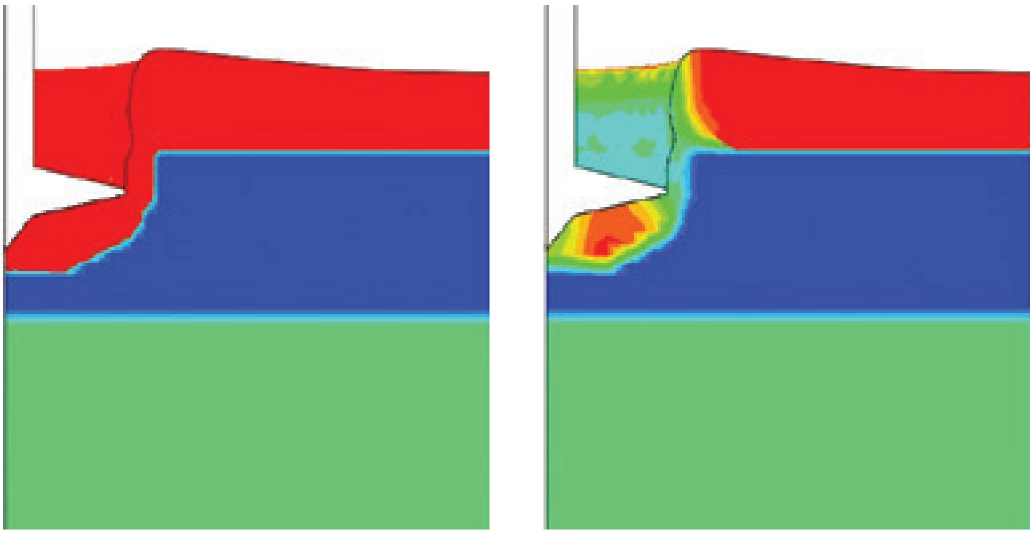

Figure 41: Contour of undrained shear strength of clay during spudcan penetration